ELSEVIER

S0032-3861(96)00600-3

Polymer Vol. 38 No. 5, pp. 1035–1045, 1997

0032-3861/97/$17.00 + 0.00

Molecular dynamics simulations of the transport of water–ethanol mixtures through polydimethylsiloxane membranes

Lydia Fritz and Dieter Hofmann*
GKSS Research Center Geesthacht, Institute of Chemistry, Kantstr. 55, D-14513 Teltow, Germany
(Received 5 February 1996; revised 10 April 1996)

Molecular dynamics (MD) computer simulation studies are conducted to examine important aspects of the pervaporation process. As a model system the separation of water–ethanol feed mixtures through a PDMS membrane is taken. Since it is yet not possible to model the whole membrane fully atomistically, two regions—the bulk and the interfacial region—were simulated. In the bulk region the movement of the penetrants has the character of a jump diffusion. The experimental diffusion coefficients are well reproduced. The water molecules are faster than the ethanol molecules. In spite of this, PDMS is a preferentially ethanol permeable membrane because of the great difference in the sorption behaviour. The simulations in the interfacial region reflect the preferential ethanol sorption. The ethanol molecules accumulate at the polymer-feed interface and take a favourite orientation to the hydrophobic PDMS surface. The polymer surface shows a swelling, which is dependent on the ethanol concentration of the feed. It can be shown that the behaviour at the interface polymer-feed is dominated by hydrogen bond forces.

(Keywords: molecular modelling; pervaporation; polydimethylsiloxane membrane)

INTRODUCTION

Pervaporation is a technique to separate a mixture of liquids by membranes[1]. In comparison with the distillation it is expected to be an energy saving alternative since only the permeating components of the liquid feed mixture undergo a phase transition. Polydimethylsiloxane (PDMS) is one of a few known membrane materials which has the tendency to discourage the passage of water molecules and to allow the passage of a wide range of much larger organic molecules at the same time[2,3]. Thus, the pervaporation mechanism here is probably not dominated by permeant size and shape effects, but it seems to be significantly influenced by permeant–polymer interactions at the interface polymer-feed[4,5].

In this paper we will have a look at the pervaporation of water–ethanol mixtures through PDMS membranes using the computer simulation technique of molecular dynamics (MD). Because of the limited atom number in a fully atomistic simulation[6] it is not possible to model the whole membrane. Instead two important regions of the membrane—the bulk and the interfacial region at the feed side—were modelled.

Until now there are only a few reports on MD simulations which explore the separation behaviour of the pervaporation. Only Tamai *et al.*[7–9] report on MD simulations of the diffusion process of methane, water and ethanol in PDMS and polyethylene and the calculation of the excess chemical potential of these systems by the Widom method to examine the sorption. Their MD simulations were carried out with a united atom approximation in the bulk region. They found a strong aggregation by the insertion of more than one water or ethanol molecule at the same time[7].

Generally, the simulations in the bulk region of pervaporation membrane polymers are very similar to those which were carried out for studying the phenomena of gas transport[10–14]. There the investigations of the diffusion of a penetrant molecule through amorphous polymers clearly show two types of motion[10,13,14]. For relatively long periods of time (typically a few 100 ps) the gas molecules stay in certain small regions of space. During this quasi-stationary period the permeant molecules are reflected from the thermally vibrating polymer matrix about every 1–2 ps. Thus, the penetrants just explore the occupied holes in the free volume. These quasi-stationary periods are interrupted by quick jumps from one hole into another one that is close by. The behaviour of the penetrant during such a jump event is of special interest for the examination of the diffusion process.

No MD simulations of the interfacial region were reported so far to investigate the sorption behaviour of an organic–water feed mixture on a polymer membrane surface. Some papers[15–17] treated a membrane bilayer of dilauroylphosphatidylethanolamine (DLPE) molecules and embedded water molecules to understand the origin of the hydration force. Other authors[18–20] reported MD simulations of interfaces between biologically relevant bilayers and aqueous solutions.

In contrast to gas permeation which is usually diffusion controlled, for many pervaporation systems the separation is more influenced by different levels of sorption of the

* To whom correspondence should be addressed

Table 1 Partial charges of the atoms

Molecule	Atom type	Partial charges forcefield cvff	Partial charges forcefield pcff
$[-Si(CH_3)_2-O-]_n$	Si	0.300	0.640
	O	−0.300	−0.440
	C	−0.300	−0.259
	H	0.100	0.053
H_2O	O	−0.820	−0.798
	H	0.410	0.399
$C^{\beta}H_3C^{\alpha}H_2OH^{*}$	C^{β}	−0.300	−0.159
	C^{α}	−0.170	0.027
	O	−0.380	−0.557
	H^{*}	0.350	0.424
	H	0.100	0.053

liquid components at the interface polymer-feed[1]. An example are PDMS membranes which are preferentially permeable for ethanol. They show a higher diffusion coefficient but a much lower sorption coefficient for the water than for the ethanol molecules[2]. Thus, here the behaviour of the whole membrane is dominated by the processes in the interfacial region.

In this work, we simulate the bulk region with three water and three ethanol molecules inside the PDMS and the interfacial region with two different feed mixtures. In order to examine the influence of hydrogen bond forces the simulations are carried out with and without consideration of hydrogen bonds. In the bulk region the trajectories of each penetrant molecule are examined and the jumps are inspected in detail. The diffusion coefficients are calculated and compared with published simulated and measured data. In the interfacial region the influence of the concentration of the ethanol molecules will be discussed by means of the time dependence of the density profiles and the molecular roughness of the polymer surface. In addition, the orientation of the ethanol molecules in the interface is investigated.

MODEL AND SIMULATION DETAILS

The InsightII/Discover software of Biosym Technologies was used for the construction and the atomistic simulations. Two different forcefields, the cvff[21] and pcff[22], were applied. Most simulations were carried out with the pcff forcefield since there the partial charges are in better agreement with partial charges calculated with a charge equilibration procedure (Cerius software of Molecular Simulations). All employed partial charges q_i of the atoms of the polymer and the permeant molecules are listed in *Table 1*. For both forcefields the Coulombic interactions were calculated according to

$$\sum_{i>j} \frac{q_i q_j}{\epsilon r_{ij}} \tag{1}$$

where ϵ is the dielectric constant and r_{ij} is the current distance between the atoms i and j. The forcefield parameters for the mainly used forcefield pcff are listed in *Table 2*. Cross terms which in the given context are leading only to minor corrections and which therefore also could be omitted are not shown in this table.

All calculations were performed on two IBM RS6000 workstations (models 340 and 3BT) and on the CRAY C916 of the Deutsches Klimarechenzentrum (DKRZ) in Hamburg.

In order to keep the effect of chain ends minimal, a single polymer chain per simulation box was employed. In all cases the polymer chain consisted of 220 monomer units $[-Si(CH_3)_2-O-]$ which together with the ethanol and water molecules were subjected to minimum image rectangular periodic boundary conditions. For the simulations of the volume element of the bulk region the polymer and the permeant molecules were packed together in an orthorhombic cell according to a modified Theodorou–Suter approach[23–25]. The exact packing and equilibration procedure is described elsewhere[14].

For the simulations in the interfacial region the pure polymer box and the pure feed box were packed and equilibrated separately, whereby the periodic boundary conditions are effective only in two dimensions. In the third dimension surface potentials force the nonperiodic coordinates of the constituent atoms into a layer of a given thickness which results from the other two boxlengths and the density of the system. After the refinement of each box the polymer and the respective feed box were layered onto each other. It should be noticed that all presented simulations of the interfacial region started with one and the same PDMS box.

For the polymer and the liquids the experimental densities at 300 K were used, i.e. 0.95 g cm^{-3} for PDMS[26], 0.79 g cm^{-3} for pure ethanol and 0.98 g cm^{-3} for the ethanol–water mixture (10 wt%–90 wt%)[27], respectively.

After the complete system refinement the MD production run started at 300 K. The forcefields, the cutoff distances for all nonbond interactions, the values of the dielectric constant and the utilized ensembles are listed in *Tables 3* and *4*. Newton's equations of motion were solved with a time step of 1 fs. Snapshots of the positions and velocities of all atoms were taken every 500 fs and saved in a history file. The length of all simulations was 1 ns with the exception of system III where the old feed was replaced by a new one after a simulation time of 1 ns and then the MD run was restarted for additional 800 ps.

For the evaluation of the simulations in the bulk region the paths of the penetrants through the polymer matrix were studied. Besides the detailed inspection of the different types of motion, the diffusion coefficients D were calculated from the least-square fits of the mean squared displacements of centres of mass of the penetrant molecules averaged over all possible origins,

$$D = \lim_{t\to\infty} \frac{1}{6t} < [R(t) - R(0)]^2 > \tag{2}$$

where $R(t)$ is a position of centre of mass of a penetrant at time t and $< \ldots >$ means the ensemble average.

RESULTS AND DISCUSSION

Bulk region

In the bulk region two different MD runs with different forcefields and dielectric constants were performed at 1 bar (systems I and II, see *Tables 3* and *4*). *Figure 1* shows the packed basic cell filled with all polymer and permeant atoms and the trajectories of the centre of mass of one representative water and ethanol molecule, respectively. It can be seen clearly that the water molecule is faster and undergoes more jumps during the same period of time. In *Figure 2* the displacement of these two penetrants from their initial positions is shown. Two types of motion are noticeable. During

Table 2 Parameters for the pcff forcefield

Quartic polynomial for bond stretching

$$\sum_b [K_2(b-b_0)^2 + K_3(b-b_0)^3 + K_4(b-b_0)^4]$$

Bonds	b_0 (Å)	K_2 (kJ · mol^{-1} · Å^{-2})	K_3 (kJ · mol^{-1} · Å^{-3})	K_4 (kJ · mol^{-1} · Å^{-4})
PDMS				
Si–O	1.6562	306.1232	−517.3424	673.7067
Si–C	1.9073	157.0049	−237.7023	356.0328
C–H	1.1010	345.0000	−691.8900	844.6000
Ethanol				
C–C	1.5300	299.6700	−501.7700	679.8100
C–O	1.4200	400.3954	−835.1951	1313.0142
O–H	0.9650	532.5062	−1282.9050	2004.7658
C–H	1.1010	345.0000	−691.8900	844.6000
Water				
O–H	0.9700	563.2800	−1428.2200	1902.1200

Quartic polynomial for angle bending

$$\sum_\theta [H_2(\theta-\theta_0)^2 + H_3(\theta-\theta_0)^3 + H_4(\theta-\theta_0)^4]$$

Bond angles	θ_0 (degrees)	H_2 (kJ · mol^{-1} · rad^{-2})	H_3 (kJ · mol^{-1} · rad^{-3})	H_4 (kJ · mol^{-1} · rad^{-4})
PDMS				
Si–O–Si	157.0260	9.0740	−19.5576	8.5000
O–Si–O	110.6930	70.3069	−6.9375	0.0000
C–Si–O	114.9060	23.0218	−31.3993	−924.9814
H–C–Si	111.5360	30.2481	−15.5255	0.0000
C–Si–C	114.9060	23.0218	−31.3993	24.9814
Ethanol				
H–C–H	107.6600	39.6410	−12.9210	−2.4318
C–C–H	110.7700	41.4530	−10.6040	5.1290
C–C–O	111.2700	54.5381	−8.3642	−13.0838
H–C–O	108.7280	58.5446	−10.8088	−12.4006
C–O–H	105.8000	52.7061	−12.1090	−9.8681
Water				
H–O–H	103.7000	49.8400	−11.6000	−8.000

Three-term Fourier expansion for torsions

$$\sum_\phi \{V_1[1-\cos(\phi-\phi_1^0)] + V_2[1-\cos(2\phi-\phi_2^0)] + V_3[1-\cos(3\phi-\phi_3^0)]\}$$

Dihedral angles	V_1 (kJ · mol^{-1})	ϕ_1^0	V_2 (kJ · mol^{-1})	ϕ_2^0	V_3 (kJ · mol^{-1})	ϕ_3^0
PDMS						
Si–O–Si–O	0.3000	0.0	0.3658	0.0	0.0000	0.0
Si–O–Si–C	0.0000	0.0	0.0000	0.0	−0.1300	0.0
H–C–Si–O	−1.3513	0.0	0.0000	0.0	−0.0580	0.0
H–C–Si–C	−1.3513	0.0	0.0000	0.0	−0.0580	0.0
Ethanol						
H–C–C–O	−0.1435	0.0	0.2530	0.0	−0.0905	0.0
H–C–C–H	−0.1432	0.0	0.0617	0.0	−0.1083	0.0
C–C–O–H	−0.6732	0.0	−0.4778	0.0	−0.1670	0.0
H–C–O–H	0.1863	0.0	−0.4338	0.0	−0.2121	0.0

Table 2 (Continued)

Nonbonded van der Waals interactions

$$\sum_{i>j} \epsilon_{ij}\left[2\left(\frac{\sigma_{ij}}{r_{ij}}\right)^9 - 3\left(\frac{\sigma_{ij}}{r_{ij}}\right)^6\right]$$

with $\sigma_{ij} = \left[\frac{\sigma_i^6 + \sigma_j^6}{2}\right]$ and $\epsilon_{ij} = 2\sqrt{\epsilon_i \epsilon_j}\frac{\sigma_i^3 \sigma_j^3}{\sigma_i^6 + \sigma_j^6}$

Atom types	σ (Å)	ϵ (kJ · mol^{-1})
PDMS		
Si	4.2840	0.07000
O	3.3500	0.24000
C	4.0100	0.05400
H	2.9950	0.02000
Ethanol		
C	4.0100	0.05400
O	3.5350	0.24000
H (CH_3, CH_2)	2.9950	0.02000
H (OH)	1.0980	0.01300
Water		
O	3.6080	0.27400
H	1.0980	0.01300

Table 3 System classifications

System	Region	Number of PDMS molecules	Number of water molecules	Number of ethanol molecules	Total number of atoms
I	Bulk	1	3	3	2238
II	Bulk	1	3	3	2238
III	Interface	1	460 (414)[a]	20 (38)[a]	3762 (3786)[a]
IV	Interface	1		160	3642
V	Interface	1	460	20	3762

[a] New feed after a simulation time of 1 ns

Table 4 Simulation parameters

System	Ensembles	Forcefield	ϵ	Cutoff (Å)	Boxlength $a = b$ (Å)	Boxlength c (Å)
I	NPT	cvff	2.8	11	≈30.7	≈30.7
II	NPT	pcff	1.0	12	≈30.8	≈30.8
III	NVT	pcff	1.0	12	24.5	73.3
IV	NVT	pcff	1.0	12	24.5	73.2
V	NVT	pcff	4.0	12	24.5	73.3

NPT: constant particle number–constant pressure–constant temperature
NVT: constant particle number–constant volume–constant temperature

relatively long periods of time the penetrants reside in a cavity and explore its shape thoroughly. However, the real transport process is only determined by jump events where the penetrant moves from a cavity to an adjacent cavity in a very short time compared to the residence time. During this jump a channel is opened based on the thermal fluctuation of the polymer matrix. *Figure 3* shows an image sequence of intersections of the box at the place of the penetrant during a jump of the water molecule. The fluctuation of the polymer matrix and the formation of the channel is clearly to be recognized. Besides this matrix behaviour also the magnitude and direction of the velocity of the permeant molecule must be suited. Detailed analyses of the polymer–penetrant interactions during the jump are in work.

The diffusion coefficients were calculated from the mean squared displacement as a function of time according to equation (1). The calculated values for each penetrant molecule and the respective average values are listed in *Table 5*. The diffusion coefficients clearly show the

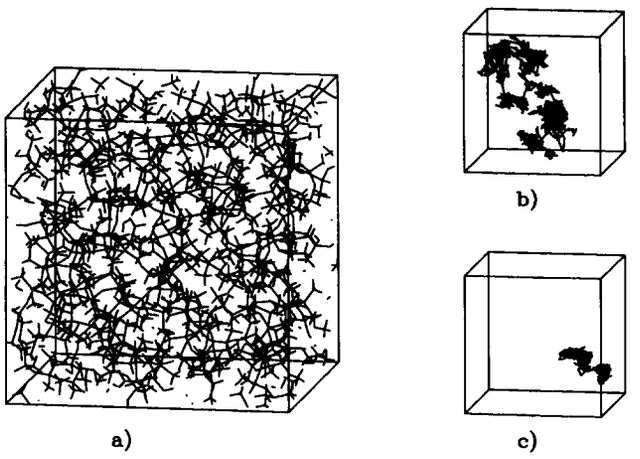

Figure 1 (a) Packed basic cell with all polymer and permeant atoms and the trajectories of a representative (b) water [H_2O(I,2)] and (c) ethanol molecule [EtOH(I,1)]. In case of (b) and (c) a boxlength of 40 Å was chosen to allow a complete representation of the trajectories

mentioned faster transport of water molecules through the amorphous PDMS membrane. Considering the still poor statistics of fully atomistic transport simulations, the values of both systems are in surprisingly good agreement with each other and with the experimental diffusion coefficients[28,29]. Similar values were obtained from Tamai *et al.*[7] for the case where they took only one penetrant molecule in the polymer matrix. Using five water or five ethanol molecules inside the PDMS they observed a formation of aggregates, which did not dissociate to single molecules during the simulation time. We could not find such a behaviour and the experimental diffusion coefficients seem to contradict the strong aggregation tendency stated by Tamai *et al.* Their calculated diffusion coefficient for the aggregated water molecules is two orders of magnitude lower than the experimental one. A further more qualitative argument for our finding consists in the fact that our interface models with complete representation of hydrogen bond forces ($\epsilon = 1$) and utilizing the pcff forcefield showed a very reasonable behaviour in the interfacial region (see below). Thus, this version of the forcefield should also give a reasonable description of the bulk behaviour. This could mean that the composed forcefield of GROMOS for PDMS and SPC/E for the water molecules used by Tamai *et al.* may perhaps overemphasize the hydrogen bonds between the solvent molecules. Otherwise a reason for the found different behaviour could also lay in the united atom approximation used by the mentioned authors.

Interfacial region

In the interfacial region simulations with two different feeds were carried out. These were on the one hand pure ethanol (system IV) and on the other hand a liquid mixture of 10 wt% ethanol and 90 wt% water (systems III and V).

In order to examine the influence of the hydrogen bond forces the second feed mixture was simulated with two different values of the dielectric constant $\epsilon = 1$ and $\epsilon = 4$ (see *Table 4*) resulting in a complete and a strongly underestimated consideration of hydrogen bonds, respectively. (Note: the biosym pcff and cvff forcefields consider hydrogen bonding only implicitly via modification of the Lennard–Jones and electrostatic potentials. Thereby $\epsilon = 1$ is necessary for a correct hydrogen bond description.) The differences after a few hundred picoseconds of simulation time are very considerable. In system III the ethanol molecules of the feed mixture accumulate at the hydrophobic polymer surface while the water molecules are prevented from reaching the polymer. This seems to be a quite reasonable behaviour considering the experimental fact that the investigated pervaporation process is solubility controlled. In system V, however, the water molecules predominantly go in the polymer–feed interface, i.e. the correct inclusion of hydrogen bonds is a decisive factor for the simulation of the interfacial region. Since the simulation of system V leads to a complete failure we will not discuss the results of that system in detail. It should be, however, emphasized that the behaviour at the interface polymer-feed is—in contrast to the behaviour in bulk—dominated by the hydrogen bond forces.

Figures 4 and *5* show the normalized density profiles of system III at the beginning of the simulation and after a

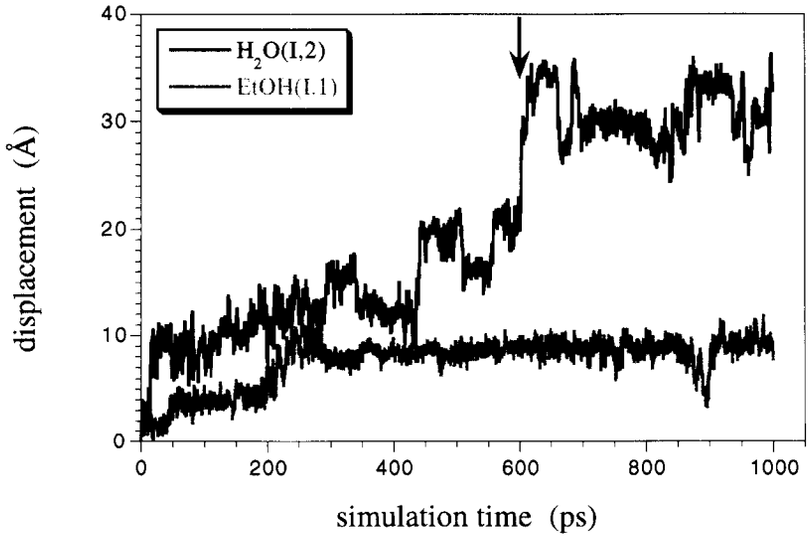

Figure 2 Displacement of the water and the ethanol molecule of *Figure 1* from their initial positions. The arrow corresponds to the time of the jump of the water molecule of *Figure 3*

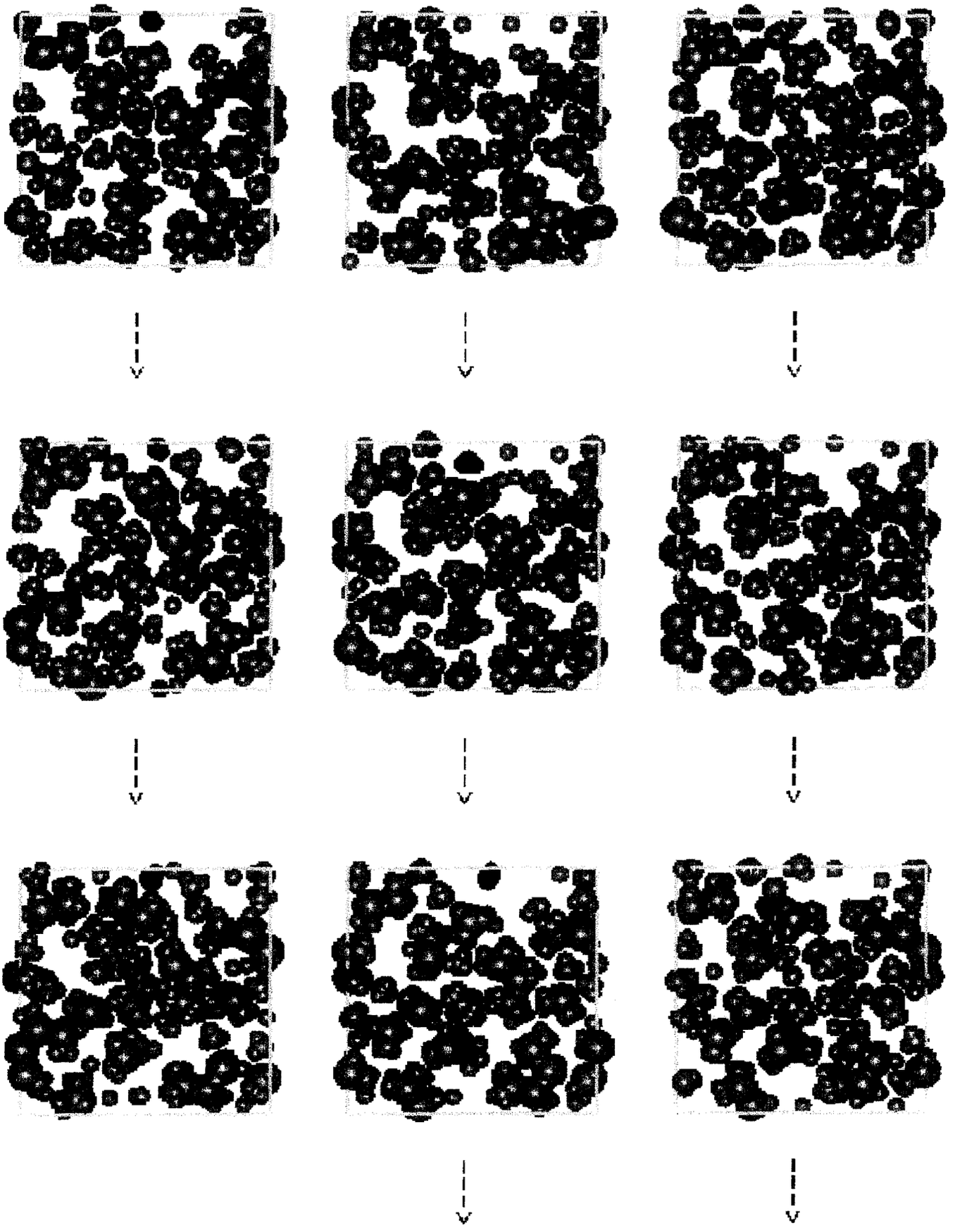

Figure 3 Intersections of the box of system I at the place of the water molecule $H_2O(1,2)$ during a simulation time period from 601.5 ps to 605.5 ps with a timestep of 0.5 ps. Grey: polymer matrix; black: jumping water molecule

Table 5 Diffusion coefficients calculated by molecular dynamics at 300 K and from experiment at 298 K

System	Penetrant	D_{sim} (10^{-5} cm^2 s^{-1})	$< D_{sim} >$ (10^{-5} cm^2 s^{-1})	D_{exp} (10^{-5} cm^2 s^{-1})
I	H_2O(I,1)	0.8		
	H_2O(I,2)	1.6	2.0	1.45 (ref. 28)
	H_2O(I,3)	3.7		2.0 (ref. 29)
	EtOH(I,1)	0.11		
	EtOH(I,2)	0.11	0.09	0.45 (ref. 28)
	EtOH(I,3)	0.06		
II	H_2O(II,1)	1.8		
	H_2O(II,2)	1.3	1.3	1.45 (ref. 28) 2.0 (ref. 29)
	H_2O(II,3)	0.9		
	EtOH(II,1)	0.11		
	EtOH(II,2)	0.38	0.44	0.45 (ref. 28)
	EtOH(II,3)	0.82		
Ref. 7	H_2O(free)		1.53	
	H_2O(aggregate)		0.025	
	EtOH(free)		0.20	
	EtOH(aggregate)		0.005	

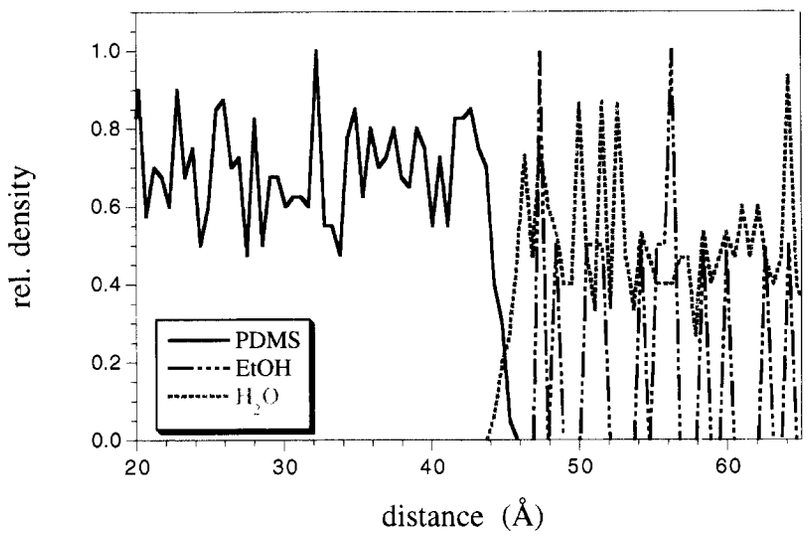

Figure 4 Density profiles of system III at the beginning of the simulation (the profiles are obtained from the starting structure)

simulation time of 1 ns. (Remark: *Figure 4* is more noisy than *Figure 5* because *Figure 4* considers just the starting structure of the system while in the case of *Figure 5* an average over 41 snapshots after 1 ns was taken. In all shown normalized density profiles the maximum density values of each participant are set to one for the sake of a better comparability.) At the beginning the feed components are mixed statistically and the boundary between polymer and feed is artificially sharp. During the simulation time the ethanol molecules of the feed enrich at the polymer surface which shows a slight swelling behaviour. Inside the feed the water and the ethanol molecules segregate almost completely and thus, a new interface is developed. After the simulation time of 1 ns only one ethanol molecule is still observed in the water region. The other 19 ethanol molecules stay in the interfacial region of polymer-feed.

It should be noticed that during the available limited simulation time it is not possible to reach the equilibrium swelling state of the polymer. Nevertheless the right tendency of the adsorption behaviour can be observed which is the main reason for the solubility. In case of a strongly swelling polymer a third region should be explored which would contain the maximum possible amount of solvent molecules. For the investigated polymer–solvent system such an examination is not required since PDMS has a comparatively low degree of swelling in contact with ethanol–water mixtures.

The normalized density profile of system IV after a simulation time of 1 ns is shown in *Figure 6*. In comparison

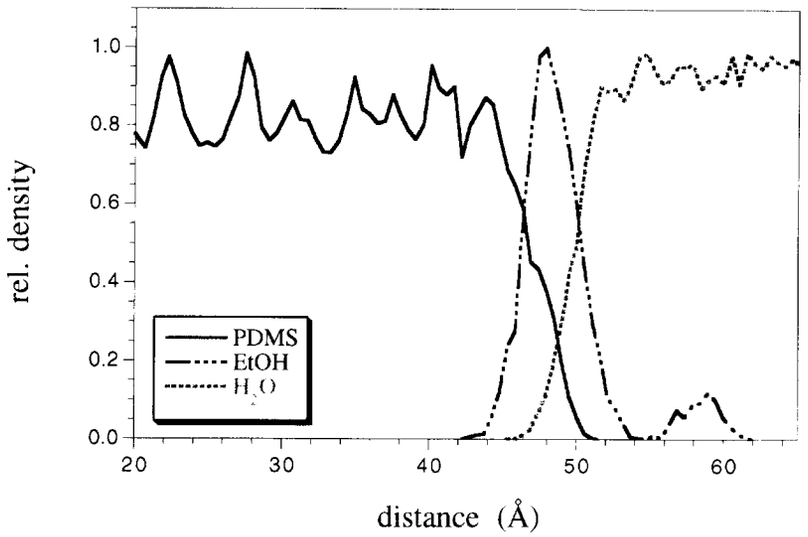

Figure 5 Density profiles of system III after a simulation time of 1 ns (the profiles were an average over 41 snapshots from 980–1000 ps)

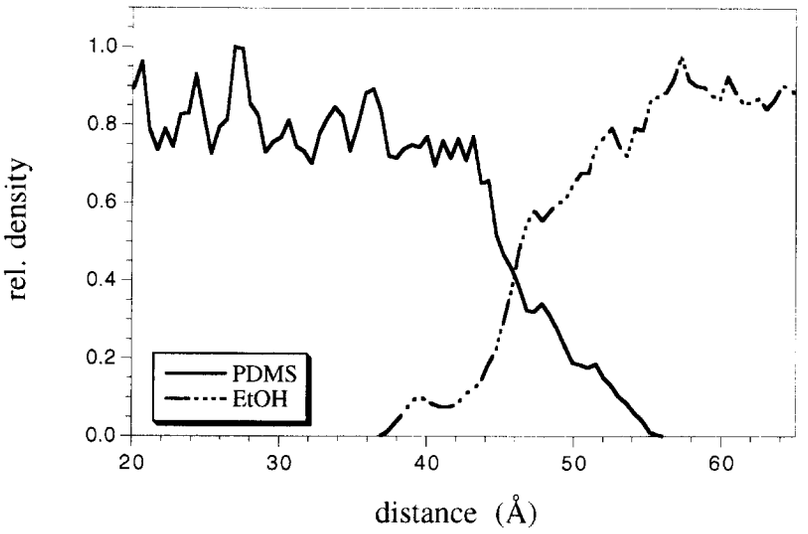

Figure 6 Density profiles of system IV after a simulation time of 1 ns (the profiles were an average over 41 snapshots from 980–1000 ps)

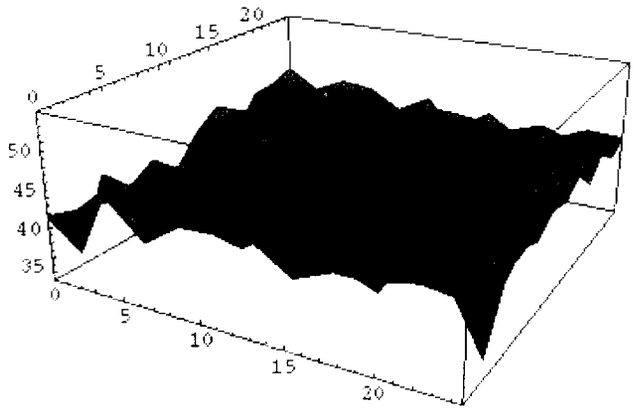

Figure 7 Surface plot of the polymer at the beginning of the simulation of systems III and IV

with system III (see *Figure 5*) in system IV a stronger swelling of the polymer interface appears. Thus, the concentration of the ethanol molecules inside the feed influences the dynamics of swelling of the polymer severely, the presence of water decreases the swelling of the polymer. This behaviour can also be recognized in the molecular roughness of the polymer surface. *Figure 7* displays the polymer surface of both systems at the beginning of the simulations and *Figures 8a, b* and *9a, b* show the swollen polymer surfaces of system III and system IV after a simulation time of 200 ps and 1 ns, respectively. The pictures were made with the help of the maximum c-coordinates of the polymer atoms in the box. The calculation was carried out by means of a grid in the ab-plane with an edge length of 1.5 Å. The 3D graphics were constructed with the Mathematica software of Wolfram Research. The grey scale of the figures reaches in both cases from black at $c = 32$ Å to white at $c = 54$ Å. Only for *Figure 9b* is the whole grey scale necessary. A distinct difference between systems III and IV appears already after a few hundred picoseconds of simulation time. The molecular roughness of the polymer surface in case of system IV is more pronounced and earlier to be recognized.

In order to examine the influence of the ethanol concentration on the swelling behaviour in more detail, the ethanol-depleted water phase of the feed outside the interface polymer–ethanol in system III was replaced

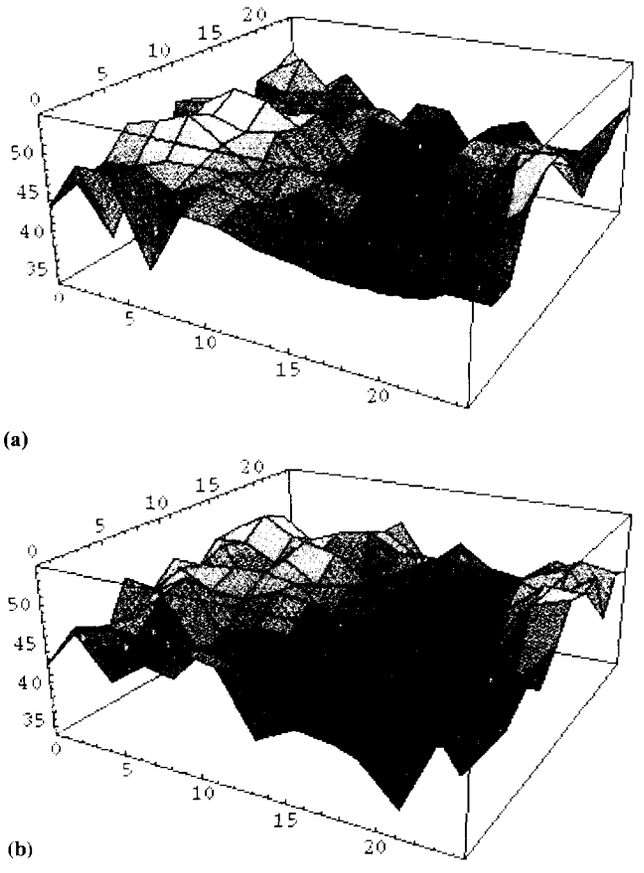

Figure 8 Surface plot of the polymer of system III after a simulation time of (a) 200 ps and (b) 1 ns

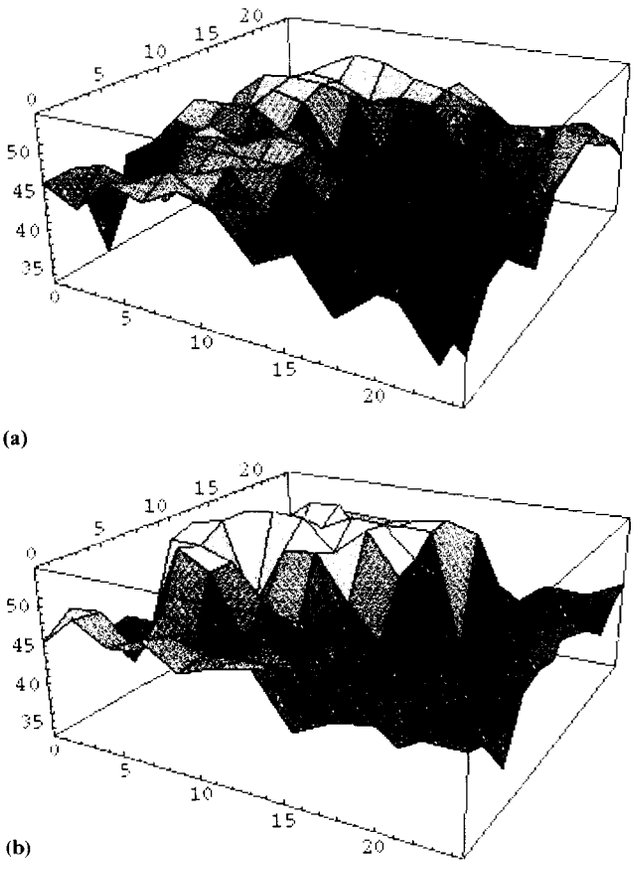

Figure 9 Surface plot of the polymer of system IV after a simulation time of (a) 200 ps and (b) 1 ns

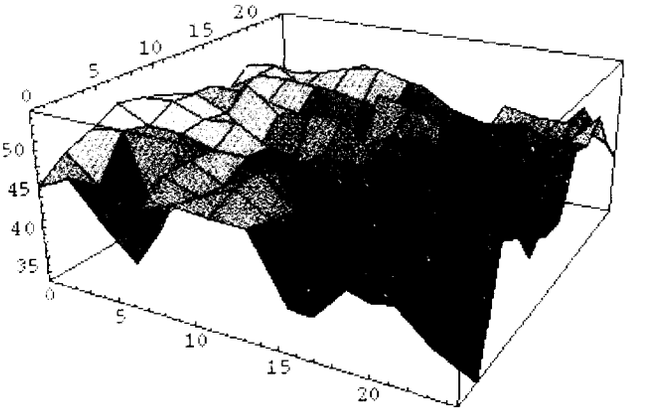

Figure 10 Surface plot of the polymer of system III after additional 800 ps of simulation time with the new feed

after 1 ns by a new feed with the original starting composition (10 wt% ethanol and 90 wt% water), i.e. additional ethanol was provided. This simulation experiment attempted to approach the reality where the feed in an almost constant composition continuously overflows the membrane surface. In the restarted MD run the same behaviour as before occurs. The added ethanol molecules move to the polymer-feed interface and thus in the existing ethanol layer. The thickness of this layer grows on and the swelling of the polymer increases. But after an additional 800 ps of simulation time with the new feed, the swelling and the molecular roughness of the polymer surface (see *Figure 10*) are still smaller than for the pure ethanol case (system IV) after the first 1 ns.

These more qualitative considerations can be quantitatively described by means of a RMS (root mean squared) value which is a common parameter to describe the roughness of the surface determined by atomic force microscopy (AFM) measurements[30]. The RMS values were calculated according to

$$\mathrm{RMS} = \sqrt{\frac{\sum_i (c_i - c_{\mathrm{ave}})^2}{N}} \qquad (3)$$

where c_i is the ith c-coordinate of the polymer surface, c_{ave} is the average of all c-coordinates of the polymer surface and N is the number of c-coordinates of the polymer surface. Because of the small number of N by the simulated systems all calculated RMS values have relatively high standard deviations. Nevertheless the same tendency can be observed as described above. At the beginning of the simulation the RMS value is ≈2.6 Å for both systems. After a few picoseconds of simulation time the RMS values of both systems increase quickly and amounts for example after 40 ps to about RMS ≈3.7 Å. Distinct differences between both systems can be recognized after a longer simulation time. Thus, for example, after a simulation time of 1 ns the RMS value for system III is ≈4.0 Å whereas for system IV a RMS value of ≈4.9 Å is calculated. After replacing the water phase of system III against the original composition and restarting the simulation for an additional 800 ps the RMS value increases to ≈4.5 Å.

In order to examine the ethanol layer in more detail the orientation of the hydrophobic and hydrophilic parts of the ethanol molecule relative to the polymer surface is explored. For this investigation two different vectors are

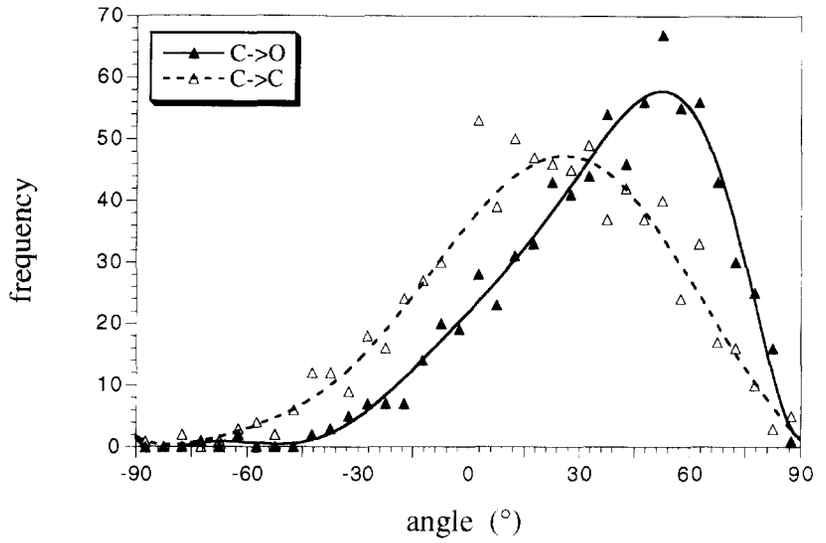

Figure 11 Distribution of the angle of two selected vectors inside the ethanol molecule to the polymer surface for system III after a simulation time of 800 ps (see text)

considered. The first one goes from one carbon atom to the other, whereby the β-carbon atom was taken as origin. The other vector goes from the α-carbon atom to the oxygen atom. In this case the origin is the position of the α-carbon atom. As a model polymer surface an *ab*-plane was taken. The vectors were calculated for all ethanol molecules at the interface for various time periods of 20 ps (41 snapshots, see model and simulation details) after the formation of the ethanol layer. The orientation of both vectors always shows a monomodal distribution (see *Figure 11*), where an angle of 0° corresponds to a vector in the plane. In the case of the C–O bond nearly all vectors have a positive angle to the polymer surface. Thus, the carbon atoms are closer to the hydrophobic PDMS surface while the oxygen atoms are closer to the hydrophilic water layer. The maximum of the distribution lays at an angle of about 52°. A similar behaviour shows the C–C vector whereby the distribution is broader and shifted to lower angles. Most vectors still have positive angles to the plane so that the more hydrophobic carbon atoms are on average closer to the PDMS surface. The distribution maximum is at an angle of about 25°. Therefore the favourite orientation of the ethanol molecules is strongly influenced by the hydrophobic nature of the polymer and the hydrophilic water layer. In addition to the observed right sorption behaviour this orientation of the ethanol molecules seems to be a good confirmation for the suitability of the pcff forcefield and the chosen simulation conditions.

SUMMARY

In the bulk region a good agreement between the simulated and experimental diffusion coefficients was found. The faster transport of the water molecules is well to be noticed. While the ethanol molecules stay longer in the occupied cavities of the free volume the water molecules realized more jumps during the same simulation time. The detailed observation of the jumps shows clearly the opening of channels in the polymer matrix during these events.

In the interfacial region a clear influence of the hydrogen bond forces was examined. In case of the complete consideration of the hydrogen bonds the ethanol–water feed mixture separates whereby the ethanol molecules accumulate at the hydrophobic PDMS surface. The ethanol molecules in the interfacial layer at the polymer surface show a favourite orientation where the hydrophobic parts point in the direction of the polymer and the hydrophilic parts point in the direction of the water molecules.

Also a strong influence of the ethanol concentration of the feed on the swelling behaviour was observed. The swelling of the polymer is stronger in case of the pure ethanol feed than for a feed mixture with a part of 10 wt% ethanol.

Because of the great number of permeant molecules used during the simulation in the interfacial region there is a much better statistic of the simulated results than in bulk. Thus, the simulations in the interfacial region seem to be a good method for predictions of the sorption behaviour. Since the permeability of most pervaporation systems is decided by the different sorption of the components of the feed mixture there exists a good opportunity to predict the separation properties of the whole membrane. In case of the gas permeation a prediction is more difficult[14].

ACKNOWLEDGEMENTS

We are grateful for stimulating discussions with Dr Helmut Kamusewitz and Professor Dieter Paul.

REFERENCES

1 Huang, R. Y. M. and Rhim, J. W. in 'Pervaporation Membrane Separation Processes' (Ed. R. Y. M. Huang), Elsevier Science Publishers, Amsterdam–Oxford–New York–Tokyo, 1991
2 Watson, J. M. and Payne, P. A. *J. Membrane Sci.* 1990, **49**, 171
3 Mulder, M. H. V., Oude Hendrikman, J., Hegeman, H. and Smolders, C. A. *J. Membrane Sci.* 1983, **16**, 269
4 Watson, J. M., Zhang, G. S. and Payne, P. A. *J. Membrane Sci.* 1992, **73**, 55
5 Richau, K., Schwarz, H.-H., Apostel, R. and Paul, D. *J. Membrane Sci.* 1996, **113**, 31
6 van Gunsteren, W. F. and Berendsen, H. J. C. *Angew. Chem.* 1990, **102**, 1020

7 Tamai, Y., Tanaka, H. and Nakanishi, K. *Macromolecules* 1994, **27**, 4498
8 Tamai, Y., Tanaka, H. and Nakanishi, K. *Macromolecules* 1995, **28**, 2544
9 Tamai, Y., Tanaka, H. and Nakanishi, K. *Fluid Phase Equilibria* 1995, **104**, 363
10 Sok, R. M., Berendsen, H. J. C. and van Gunsteren, W. F. *J. Chem. Phys.* 1992, **96**, 4699
11 Gusev, A. A., Müller-Plathe, F., van Gunsteren, W. F. and Suter, U. W. *Adv. Polym. Sci.* 1994, **116**, 207
12 Gusev, A. A., Suter, U. W. and Moll, D. J. *Macromolecules* 1995, **28**, 2582
13 Müller-Plathe, F. *Acta Polym.* 1994, **45**, 259
14 Hofmann, D., Ulbrich, J., Fritsch, D. and Paul, D. Submitted for publication in *Polymer* 1996, **37**, 4773
15 Berkowitz, M. L. and Raghaven, K. *Langmuir* 1991, **7**, 1042
16 Marrink, S.-J., Berkowitz, M. and Berendsen, H. J. C. *Langmuir* 1993, **9**, 3122
17 Zhou, F. and Schulten, K. *J. Phys. Chem.* 1995, **99**, 2194
18 Berlepsch, H. von, Hofmann, D. and Ganster, J. *Langmuir* 1995, **11**, 3676
19 Nicklas, K., Böcker, J., Schlenkrich, M. Brickmann, J. and Bopp, P. *Biophys. J.* 1991, **60**, 261
20 Egberts, E., Marrink, S.-J. and Berendsen, H. J. C. *Eur. Biophys. J.* 1994, **22**, 423
21 Lifson, S., Hagler, A. T. and Dauber, P. *J. Am. Chem. Soc.* 1979, **101**, 5111
22 Sun, H., Mumby, S. J., Maple, J. R. and Hagler, A. T. *J. Am. Chem. Soc.* 1994, **116**, 2978
23 Theodorou, D. N. and Suter, U. W. *Macromolecules* 1985, **18**, 1467
24 Theodorou, D. N. and Suter, U. W. *Macromolecules* 1986, **19**, 139
25 Polymer User Guide, Amorphous Cell Section, version 6.0 San Diego: Biosym Technologies, 1993
26 'Silicones and Silicon-containing Polymers', ABCR-Catalog 1994/95
27 'Chemiker-Kalender, 3. Aufl.' (Ed. by C. Synowietz and K. Schäfer), Springer-Verlag, Berlin, Heidelberg, New York, Tokyo, 1984
28 Okamoto, K., Nishioka, S., Tsuru, S., Sasaki, S., Tanaka, K. and Kita, H. *Kobunshi Ronbunshu* 1988, **45**, 993
29 Watson, J. M. and Baron, M. G. *J. Membrane Sci.* 1995, **106**, 259
30 Fritzsche, A. K., Arevalo, A. R., Moore, M. D. and O'Hara, C. *J. Membrane Sci.* 1993, **81**, 109